Chapter 6

The spectral tuning of photoisomerization of 11-*cis* retinal in conjugation with Au_{14}: a theoretical outlook

Abstract

Being the intrinsic property of gold nanocluster, the localised surface plasmon resonance (LSPR) leads to an enhancement of absorption of retinal molecule, while conjugated to Au_{14} nanocluster. This enhanced absorption of retinal has been revealed as the rationale for the raise of photoisomerization of retinal from visible to infrared region. The photoisomerization process is recognized as the triggering step of vision. Hence this shifting of photoisomerization has been presumed to adjust the visual response. The Au_{14} nanocluster motifs are varied through O_h, D_{2h} and C_{4v} symmetries, to obtain preeminent spectral shifting of photoisomerization. The constructive interference of the transition dipole moments (TDMs) in retinal-gold nanoconjugates makes the Au_{14} nanocluster with D_{2h} symmetry, the most efficient enhancer for the upgrading of photoisomerization. The conjugation of isolated retinal with gold probes makes the process of 11-*cis* to all-*trans* isomerization thermodynamically more favorable, as evidenced through thermochemical and vibrational frequency analysis. The entire evaluation recommends to a speculation as if gold nanoprobes may be used as vision enhancer.

6.1 Introduction

Due to the presence of surface plasmon resonance (SPR) property, metal nanoparticles (NPs) bestow multifarious applications, spanning the fields of optics and photonics to biomedical applications.[1-5] The localized surface plasmon resonance (LSPR) associated with the NPs develops a strong electromagnetic near field enhancements, that is responsible for surface enhanced spectroscopic properties like absorption, fluorescence, scattering, Raman scattering, in the proximity of the metal NP.[6] When a molecule resides near the metal NP, it experiences a greater capacity to absorb photons. This leads to dramatic enhancement in the electronic excitations, known as surface-enhanced absorption of molecules, linked to NPs. This enhanced absorption of molecules has been interpreted by several theoretical approaches. The time-dependent density functional theory (TDDFT) has been found to play a significant role in explaining this phenomenon from the perspective of electronic transition between molecular states.[7-8] Recently the electronic excitation has been interpreted as density oscillations in spite of electronic transition between distinct molecular states, in support of TDDFT studies.[9-10] Thereby TDDFT has been implemented in the present theoretical investigation to interpret the enhanced excitations of molecules arising from the SPR of NPs. Relevant researches in the field of enhanced absorption have been explored for several systems such as dyes rhodamine B and nile blue on Au and Cu films,[11] tryptophan-silver cluster system,[12,13] merocyanin dyes near silver and copper NPs[14] etc. through TDDFT studies. The TDDFT study applied to tryptophan-silver cluster system[12] as well as complexes of both di- and tri-peptides with silver clusters[15,16] demonstrated the reason behind the enhanced absorption experienced by the biomolecules in the vicinity of NPs. Pursuing this concept of enhanced absorption of molecules near NP, a theoretical endeavor has been taken to explore optoelectronic properties of retinal while conjugated to plasmonic NP and its relevant implementations in biomedical applications. A rational selection of retinal molecule is made due to its involvement in a complicated photo-biochemical process, called vision.

Vision in human eye utilizes retinal for the conversion of electromagnetic energy into electrochemical energy. Retinal is the photo-absorbing chromophore that resides in the photo-receptor protein rhodopsin. The photoisomerization of 11-*cis*-retinal to the all-*trans* retinal

(Figure 1), is the first step in the process of vision to trigger electrochemical signal of visual response.[17-21] The maximum absorbance wavelength of 11-*cis* retinal is 500 nm (the green part of the spectrum),[22] which initiates the process of photoisomerization of retinal. Plenty of theoretical works have been carried out to explain the exact molecular mechanism of the spectral shift in retinal in different environments. Thorough investigation on optoelectronic properties of retinal has been made by Merchán *et al.*, who have studied the electronic spectrum of all-*trans* retinal and its truncated models by *ab initio* method.[23] At low temperature, the photochemistry of 11-*cis*-retinal and its mechanism of photoisomerization are also investigated.[24] Send *et al.* have explored theoretically the lowest excited states of 11-*cis*-retinal by coupled cluster method.[25] On the other hand, quantum chemical study have also been performed on electronic and structural properties of all- *trans* retinal and its aromatic analogs.[26] Recently, the effect of protein environment on the photo excitation properties of retinal has been investigated experimentally and theoretically,[27,28] which reveals the key interactions involved in the color-shifting process. On the other hand, recently a great interest has been developed to understand and control the photoresponsive behavior of the chromophores deposited on metallic surface or nanoparticles.[29] Therefore retinal has been considered as the molecule of interest in the present work.

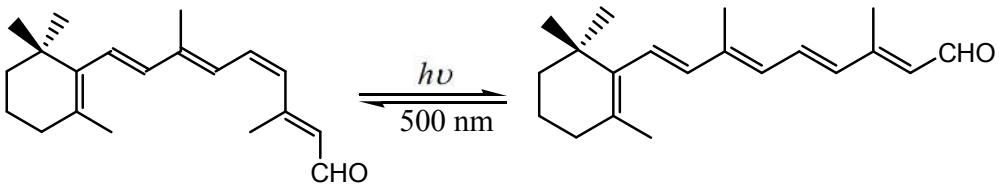

11-*cis*-retinal all-*trans* retinal

Figure 6.1 Photoisomerization of 11-*cis*-retinal to *all-trans* retinal by photo-absorption at 500 nm wavelength.

Retinal molecule in the proximity of plasmonic NPs is expected to exhibit enhanced absorption property. This enhanced absorption is presumed to shift the spectral occurrence of photoisomerization of 11-*cis* retinal. The spectral shift of photoisomerization may have an extensive influence in the process of vision as it is the triggering step of the entire mechanism of visual response. Thus adjustment of vision can be achieved through tagging the plasmonic NP to the retinal chromophore.[30,31] It has been explored that NP based drug delivery systems (DDS)

may be a superior replacement of eye drops or ointments due to its excellent efficacy and safety for ophthalmic treatment.[32-36] The NP-based DDS offers the opportunity to develop the environment of plasmonic NP near retinal molecule. Nanoparticles based on several metals such as gold, silica, silver, lanthanides,[37, 38] and quantum dots based on CdSe, ZnS, PbSe, ZnSe, and ZnS play a substantial role in biology and medicine because of their unique size dependent optical properties.[39,40] However for having the feature of human toxicity and cytotoxicity, semiconductor nanomaterials are prohibited for in vitro and in vivo applications. In contrast to that colloidal gold NPs (Au NPs) are found as an important substitute due to their potential noncytotoxic, facile immunotargeting features.[41] More over Colloidal gold nanoparticles have been widely used for drug delivery, imaging, biomedical diagnostics, and therapeutic applications due to their stability, biocompatibility, very high surface area, ease of preparation, characterization and so on.[42-44] Hence gold NPs become the ideal alternative for their nontoxic nature to retinal and optic nerves.[45] The Au NPs can be made biocompatible through the functionalization of their surface which shows a strong affinity for the –SH and $–NH_2$ group.[46] Another advantage of gold NPs is that they exhibit the plasmon resonance near the absorbance wavelength of the retinal.[36] Thus gold NP emerges as perfect probe for conjugation with 11-*cis*-retinal to carry forward the present investigation.

In this work, we carry out a detail theoretical investigation on the molecular mechanism of spectral shift of 11-*cis*-retinal in the vicinity of gold NPs. The clear understanding of the photo responsive behavior of NP-chromophore conjugate is expected to provide valuable information for the latest ophthalmic treatments. Several gold nanoclusters such as thiolate protected Au_{20}, Au_{23}, Au_{24}, Au_{25}, Au_{28}, Au_{30}, Au_{36}, Au_{38}, Au_{102}[47-56] and phosphine protected Au_{14}, Au_{20}, Au_{22}, Au_{39}[57-61] as well as mixed ligand (both thiolate and phosphine) protected Au_{24}, Au_{25}[62] have been reported till date. In the present work, our concern is about Au_{14} cluster as it has been found to possess highest binding energy per atom.[63] A very recent report on the fabrication of Au_{14} cluster also indicates its actual existence as stabilized nanocluster.[64] Therefore a performance of quantum chemical calculations has been carried out on the systems of Au_{14} nanoclusters conjugated to 11-*cis* retinal. Recently it has been shown that the photo responsive behavior can be tuned by changing the shape and size of the nanoclusters.[65] As symmetry is one of the key descriptors of 3D shapes,[66-68] it is considered as main variable to tune the optical properties of

retinal-cluster conjugates. The considered symmetries are O_h, D_{2h} and C_{4v} corresponding to their shapes like cube, rod and cone respectively. This theoretical venture has been executed through excitation energy analysis of the retinal-cluster conjugates along with the isolated gold clusters and 11-*cis*-retinal individually using TDDFT approach. The corresponding excited states have also been estimated for further clarification. Finally the thermochemical and vibrational frequency analysis are carried out to validate the feasibility of photoisomerization of 11-*cis*-retinal upon conjugation with gold nanoprobes. The overall protocol has successfully addressed the molecular mechanism of spectral shift of retinal in the proximity of gold.

6.2 Computational details and methods:

Most of the calculations are carried out using the Amsterdam Density Functional (ADF 2010.02) program package.[69,70] The ground states of each system and the excited states of retinal-cluster conjugates are optimized using GGA (Generalized Gradient Approximation)[71] based functional BLYP.[72,73] The Slater type triple-ζ polarized (TZP) basis set has been used. The gold clusters are optimized within the scalar relativistic zeroth-order regular approximation (ZORA)[74-76] employing *4f* frozen core TZP basis set. The full geometry optimization of ground and excited states of retinal-gold nanoconjugates is performed employing the same functional and basis set as used for individual components. A systematic analysis of the excitation energies of isolated 11-*cis*-retinal, gold clusters and retinal-gold conjugates is performed with the time dependent density functional theory (TDDFT), using BLYP exchange-correlation functional,[77] coupled with LB94 potential for adequate estimation of esxcitation.[78] The basis set employed in this computation is kept similar to that used in geometry optimization process. Recently the DFT functional CAM-B3LYP has been proved to be consistent for long range correction effects often encountered in the calculation of charge transfer of molecules.[79] The UV-visible spectra for the retinal-cluster conjugates have been calculated by performing single point time dependent TDDFT calculations with the long range corrected CAM-B3LYP functional using LANL2DZ basis set.[80-82] These tests have been performed to confirm the charge transfer characteristic of the electronic transition of the conjugates involved in the present work. The functional CAM-B3LYP has not been implemented in the local version of ADF. Therefore the calculations have been carried out using the Gaussian 09 program.[83] Finally, the vibrational frequencies are

obtained through analytical second derivatives implementation in ADF.[84,85] Enthalpies at 298.15 K and 1 atmosphere (H_{298}) were calculated from electronic bond energies (E) and vibrational frequencies using standard thermochemistry relations for ideal gas[86] according to the following equation:

$$\Delta H_{298} = \Delta E_{\text{trans},298} + \Delta E_{\text{rot},298} + \Delta E_{\text{vib},0} + \Delta\left(\Delta E_{\text{vib},0}\right)_{298} + \Delta(pV). \qquad (6.1)$$

Here $E_{\text{trans},298}$, $E_{\text{rot},298}$, and $E_{\text{vib},0}$ are the differences between the reactant and the product in translational, rotational, and zero point vibrational energy respectively; ($E_{\text{vib},0})_{298}$ is the change in the vibrational energy difference from 0 to 298.15 K change in temperature. The vibrational energy corrections are based on our frequency calculations. The molar work term (pV) is (n)RT. The thermal corrections for the electronic energy are neglected.

6.3 Results and Discussion

Light induced isomerization of photochromic retinal is one of the fastest processes in nature, taking place on a femtosecond timescale.[87] In the entire mechanism of vision (depicted in Scheme 6.1), only the Step 2 emerges as the triggering step, can be manipulated when the chromophore has been tagged with gold nanoprobe. Due to the inherent accumulation of LSPR property of the gold nanoprobe, it can be possible to promote the spectral shift of photoisomerization. Hence the underlying theme of the present work is to explore the effect of LSPR of gold nanocluster on the molecular mechanism of photoisomerization of retinal.

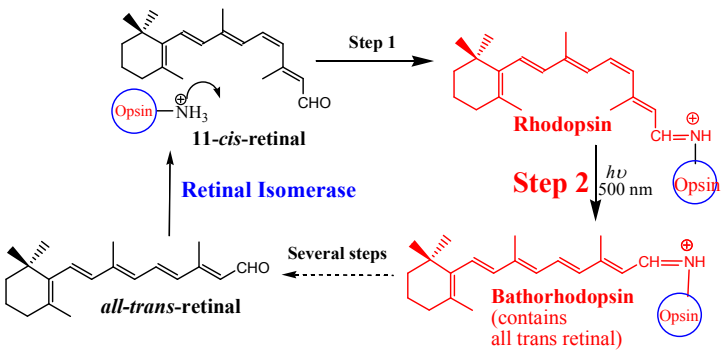

Scheme 6.1 Schematic representation of the primary steps in the mechanism of vision.

6.3.1 Analysis of photoexcitation

The optimized geometry of 11-*cis*-retinal, considered for excitation study, is found to be in close agreement with the experimental XRD data (Figure S1 in the supporting information).[88] Besides that, the optimized parameters (specially Au–Au distance) of the gold clusters with different symmetries (O_h, D_{2h} and C_{4v}), vary from 2.87 Å to 3.11 Å according to their position from internal to peripheral which is also found to be in well agreement with reported data.[89,90] The absorption spectra of 11-*cis*-retinal, obtained through TDDFT, appears with two distinct peaks at 389 nm and 500 nm [Figure 6.2(a)], which are concordant with reported values (Table 6.1).[23, 91] The second peak at 500 nm corresponds to the transition from highest occupied molecular orbital (HOMO) 57A (π bonding) to lowest unoccupied molecular orbital (LUMO) 58A (π* antibonding) as represented in Figure 2b. This π-π* transition has been considered as a significant step leading to the photoisomerization of rhodopsin (11-*cis* form) to bathorhodopsin (*all-trans* form).[92]

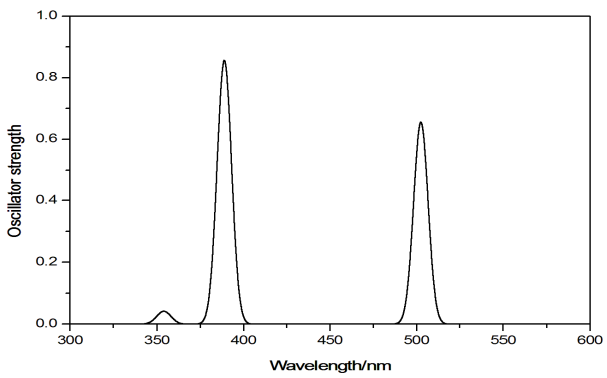

(a)

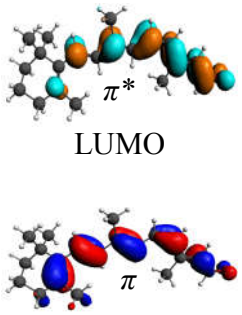

(b)

Figure 6.2 (a) TDDFT valence excitation spectra (oscillator strength vs excitation energy) of 11-*cis*-retinal molecule. **(b)** The representation of MOs participating in π-π* transition leading to photoisomerization of 11-*cis*-retinal to all-*trans* retinal at 500 nm.

The HOMO-LUMO energy gap ($E_{HOMO\text{-}LUMO}$) corresponding to this transition is found to be 1.74 eV (Table 6.1), which is approximately equal to the reported value of π-π* transition energy, 2 eV.[93] This subtle difference in the absorption energy may be attributed to the protein environment, which is not considered in the present calculation. Next, the optimized gold

nanoclusters (Au_{14}) with different symmetries (i.e. O_h, D_{2h} and C_{4v} in Figure 6.3) are considered for excitation energy study.

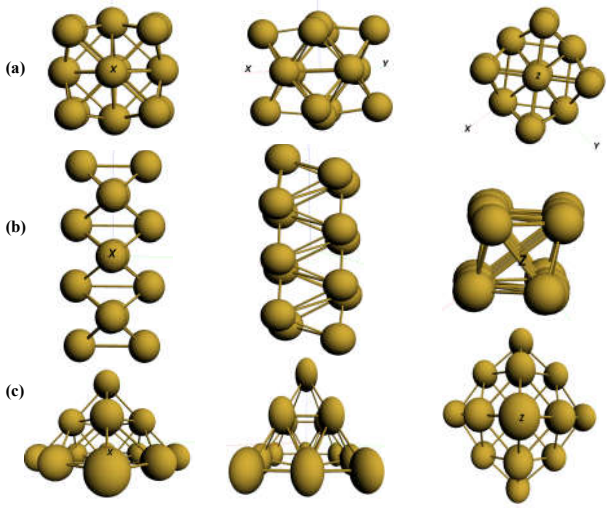

Figure 6.3 Optimized Au_{14} clusters with **(a)** O_h, **(b)** D_{2h} and **(c)** C_{4v} symmetries respectively.

The excitation energies of the gold nanoclusters are found approximately close to the reported values (Table 6.1 and Figure 6.4) irrespective to their symmetries.[94,95] The trend of the excitation energies with respect to symmetries has also been compared with that of experimental data exhibited by synthetic gold nanoclusters having shapes (cube, rod and cone) corresponding to relevant symmetries (O_h, D_{2h} and C_{4v}). This brings a good correspondence between the calculated and reported trend mentioned in Table 6.1. This resemblance of computed and experimental values of isolated retinal along with gold nanoclusters, thus solicits for the validity of adopted methodology.

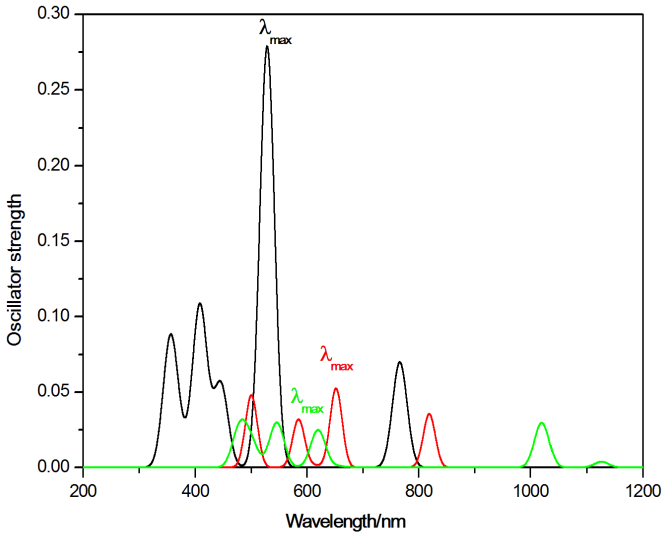

Figure 6.4 The most intense excitations (λ_{max}) for Au_{14} clusters having O_h, D_{2h} and C_{4v} symmetries, are depicted in black, green and red colors respectively.

Table 6.1 Discrete electronic excitation of 11-*cis*-retinal and its gold conjugates with different symmetries calculated using TDDFT. (Superscripts to the numerical values in the last column indicate corresponding references).

Systems	**Au_{14} Symmetry**	**Spectra**	**Source MO**	**Destination MO**	**$\Delta E_{occ\text{-}vir}$ (eV)**	**Oscillator strength**	**Excitation Energy (eV)**	**Wavelength (nm)**	**Reported wavelength (nm)**
11- *cis*-Retinal	---------	Peak @ 500 nm (Figure 2a)	57A (HOMO)	58A (LUMO)	1.738	0.656	2.46	500	500[23,91,96]
Au_{14}	O_h	λ_{max} (Figure 4)	10T2.g (HOMO)	13T1.u (LUMO+3)	2.111	0.279	2.346	528	500[94,95], 540 545[29]
	D_{2h}	λ_{max} (Figure 4)	16B3.g (HOMO −5)	19B2.u (LUMO)	2.244	0.03	2.272	545	500[94,95], 510 540[97]
	C_{4v}	λ_{max} (Figure 4)	18B1 (HOMO −2)	33E1 (LUMO)	1.715	0.052	1.902	651	500[94,95], 750 1300[98]
11- *cis*-Retinal - Au_{14} conjugates .	O_h	λ^{A}_{max} (Figure 6)	189A (HOMO −1)	191A (LUMO)	0.418	0.025	0.454	2726	
	D_{2h}	λ^{B}_{max} (Figure 6)	188A (HOMO −2)	192A (LUMO+1)	0.481	0.113	0.563	2200	
	C_{4v}	λ^{C}_{max} (Figure 6)	190A (HOMO)	194A (LUMO+3)	0.687	0.009	0.882	1405	

Prior to the excitation energy study of retinal-gold nanoconjugates, their ground state geometries are optimized followed by frequency calculation to check their vibrational stability. Complete list of harmonic frequencies of the ground state retinal-gold conjugates are given in Tables S6.1, S6.2, S6.3 in the supporting information. Imaginary frequencies of magnitude less than 36 cm^{-1} is attributed to the small inaccuracy in numerical grid.[99] The calculated frequencies of retinal-gold conjugates are found close to the reported values.[100] The most intense excitation peaks for retinal-gold conjugates with symmetries O_h, D_{2h} and C_{4v} (designated as λ^A_{max}, λ^B_{max}, and λ^C_{max} respectively in Figure 6.5(a) are found to be red shifted in the order $\lambda^C_{max} < \lambda^B_{max} < \lambda^A_{max}$, though all the peaks belong to the IR region. This trend corresponds to the descending value of $E_{occ\text{-}vir}$ from C_{4v} to O_h symmetry of Au_{14}-retinal conjugates (Table 1). When 11-*cis* retinal is conjugated to gold clusters, unique electronic structures develop. It has been observed that some MOs of gold cluster encounter into the gap of HOMO-LUMO of 11-*cis* retinal. This leads to a more discrete electronic distribution and thereby decreases $E_{occ\text{-}vir}$ in the conjugates (Figure S2 of supporting information). The smaller $E_{occ\text{-}vir}$ in retinal-gold conjugates thus enhances the absorption wavelength. The TDDFT analysis performed for retinal-gold conjugates reveals the nature of source and destination MOs, from and to which the excitations take place (Figure 5b). The source MOs are found to be composed exclusively of Au atomic orbitals whereas the destination MOs are identical to the LUMO of the free retinal (Figure 5b). Therefore, the most intense peaks of the retinal-gold conjugates originate from the gold to retinal charge transfer (CT) excitation in all the cases.

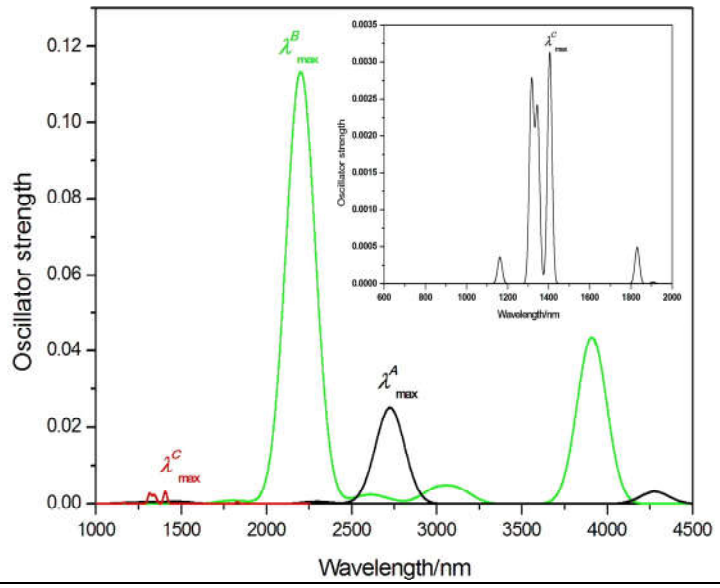

(a)

System	Source MO		Destination MO
(i)	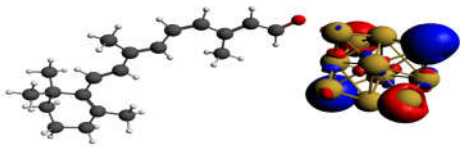 **189A(HOMO 1)**	→	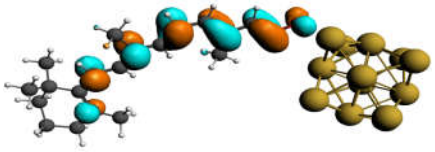 **191A (LUMO)**
(ii)	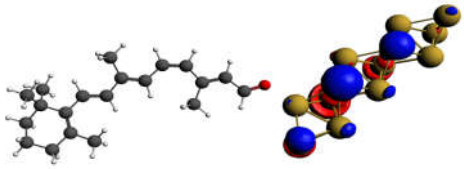 **188A(HOMO 2)**	→	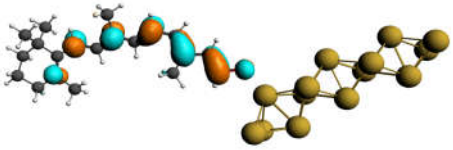 **192A(LUMO+1)**
(iii)	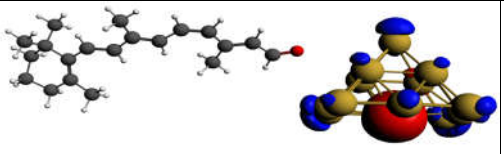 **190A(HOMO)**	→	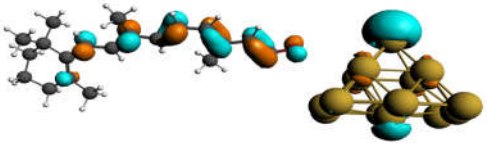 **194A(LUMO+3)**

(b)

Figure 6.5 (a) UV-visible excitation spectra with most intense excitations (λ_{max}) for retinal-cluster conjugates with symmetries O_h, D_{2h} and C_{4v} are shown in black ($\lambda^A{}_{max}$), green ($\lambda^B{}_{max}$) and red ($\lambda^C{}_{max}$) colors respectively. The peak $\lambda^C{}_{max}$ is also displayed in the inset for clarity. (b) The source and destination MOs responsible for the peaks $\lambda^A{}_{max}$, $\lambda^B{}_{max}$, $\lambda^C{}_{max}$ respectively.

For further confirmation about the CT excitation, the excitation energy calculation has been carried out using long range corrected functional CAM-B3LYP. Here also the most intense excitation peak of the retinal-gold (D_{2h}) conjugate i.e. $\lambda^{B}_{\max}$ is red shifted (Figure S6.3). The analysis of most intense peaks shows a good convergence about CT nature of excitation with the previous one. Here also the transition of electron appears from the cluster (gold) MO to the retinal MO. (Figure 6.6)

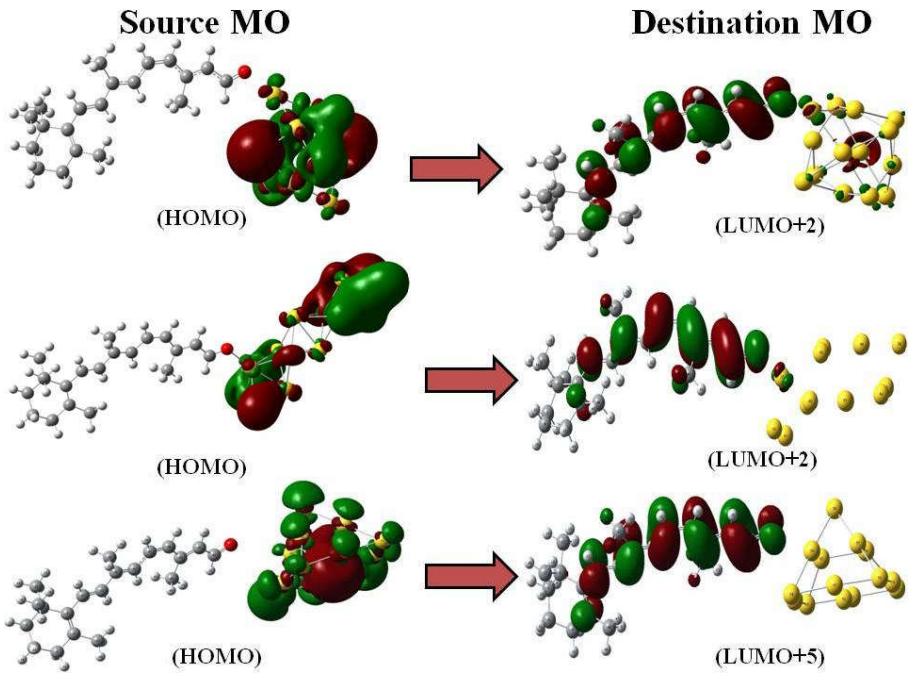

Figure 6.6 The source and destination MOs obtained from the UV-visible excitation energy calculation of the conjugates using CAM-B3LYP long range corrected functional.

To check the accountability of the role of CT excitation in photoisomerization of 11-*cis* retinal, analysis of the excited state of the conjugates corresponding to particular excitations has been carried out. The retinal-Au_{14} (C_{4v}) has not been considered due to its incomparable small value of excitation energy with respect to the other conjugates. A justification of the isomerization is revealed from a close inspection of the optimized excited state geometries,

where *trans*-retinal moiety is seen in conjugation with the Au_{14} clusters (Figure 6.7). Relevant frequency calculation has been reported in tables S4 and S5 of the supporting information.

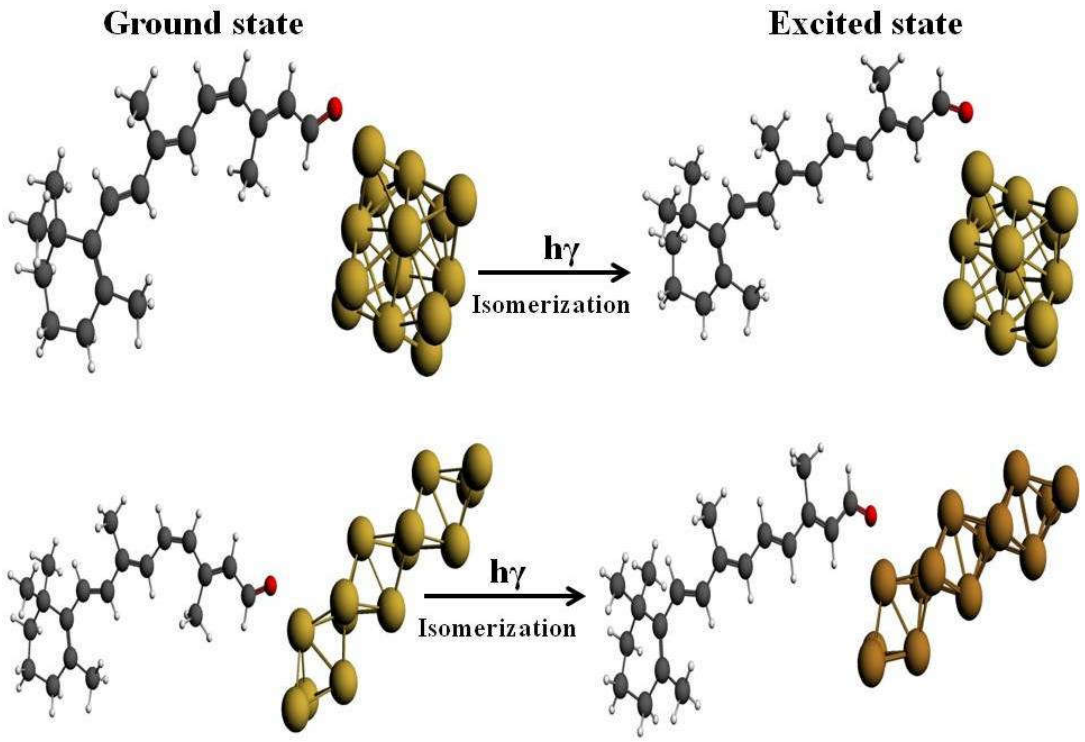

Figure 6.7 An apparent isomerization is displayed as the *cis*- retinal is transformed into *trans*-form in the estimation of the excited states corresponding to the most intense excitations for (a) retinal-gold (O_h) and (b) retinal-gold (D_{2h}) conjugates.

Comparison of the absorption maxima (λ_{max}) of free retinal and the conjugates bearing gold clusters with different symmetries also reveals an interesting difference in their oscillator strength. At a specific frequency, the peak intensity depends on the constructive or destructive interference of transition dipole moments (TDMs).[101] In case of retinal-Au_{14} (O_h) and retinal-Au_{14} (C_{4v}), the different signs of the TDMs corresponding to three major transitions (Table 6.2) suggests a destructive interference, while the same signs of principle TDMs in case of retinal-Au_{14} (D_{2h}) advocates for the constructive interference. This fact well explains the maximum oscillator strength for the conjugate of retinal with gold cluster of D_{2h} symmetry.

Table 6.2 TDDFT data most intense excitation wavelengths of 11-*cis*-retinal, gold clusters of different symmetries and corresponding retinal-gold conjugates with involved transitions and their dipole contribution to transition dipole moments.

System	λ_{max} (nm)	Transitions	Weight	Dipole contribution
Retinal-Au_{14}(cube)	2725.99	HOMO−1→ LUMO	0.984	1.343
		HOMO→ LUMO	0.014	0.071
		HOMO−2→ LUMO	0.001	0.004
Retinal-Au_{14}(rod)	2200.39	HOMO−2→LUMO+1	0.826	1.051
		HOMO→ LUMO+1	0.12	0.972
		HOMO→ LUMO+3	0.023	0.562
Retinal-Au_{14}(cone)	1405.41	HOMO→ LUMO+3	0.449	0.643
		HOMO→ LUMO+2	0.333	0.669
		HOMO→ LUMO+5	0.115	0.269

6.3.2 Feasibility of the photoisomerization of retinal-gold conjugates

Finally it becomes essential to check the thermochemical feasibility of isomerization of 11-*cis*-retinal to all-*trans* retinal in the proximity of gold cluster. Thus, the free energy change (*G*) associated with the photoisomerization of 11-*cis*-retinal is compared with that of retinal-gold conjugates to assess the spontaneity of the isomerization. The thermo chemistry analysis of isomerization of 11-*cis*-retinal to all-*trans* retinal gives the *G* value of 4.47 kcal/mole which is in good agreement with reported value of 4 kcal/mole (Table 6.3).[102] For retinal-gold conjugates, the retinal–Au_{14} (O_h) conjugate is preferred for themochemistry analysis owing to the maximum shift of its most intense excitation peak (λ^{C}_{max}) in the IR region. For retinal–Au_{14} (O_h) conjugate, the G value of 11-*cis*-retinal to all-*trans* retinal isomerization is found to be ≈ 5 kcal/mole (Table 6.3), which satisfies the criterion of spontaneity even in retinal-gold conjugates.

Table 6.3 Thermochemical data of 11-*cis*-retinal and its gold conjugate calculated from vibrational frequency analysis.

System	Total bonding energy (kcal/mole)	Total internal energy(U) (kcal/mole)	Enthalpy(H) (kcal/mole)	Free energy(G) (kcal/mole)	Free energy change(G) (kcal/mole)
11-*cis*-retinal	6308	6033.63	6034.22	6080.46	4.47
All-*trans* retinal	6313.37	6039.23	6038.64	6084.93	
11-*cis*-retinal - Au_{14} conjugate	6895.98	6601.44	6600.84	6691.85	5.33
All-*trans* retinal-Au_{14} conjugate	6900	6605.09	6604.49	6697.18	

Earlier theoretical studies have revealed the excited state isomerization dynamics of rhodopsin,[103,104] where it has been found that the ethylenic double bond (C_{11}=C_{12}) completely breaks via bicycle pedal motion.[105] This leads to decrease in the force constant of torsional oscillations around the C_{11}=C_{12} double bond and thereby decreasing the potential energy barrier of torsional oscillations with respect to the C_{11}=C_{12} bond.[93,106-107] Subsequently the observation of structural change during isomerization of 11-*cis*-retinal to all-*trans* retinal by time resolved femtosecond stimulated Raman spectra of transient photoproduct, photorhodopsin signifies the red shifting of C_{11}=C_{12} stretching frequency along with the frequency of hydrogen out of plane (HOOP) around the C_{11}=C_{12} bond.[18,108] It has been reported that the vibrational spectrum of rhodopsin includes the symmetric C=C ethylenic stretch at 1548 cm ^{1} and the HOOP wagging motion at 969 cm ^{1}.[18] In the present study the vibrational spectrum of 11-*cis* retinal corresponding to C=C stretching at 1526 cm^{-1} is lower than the reported value due to absence of the protein environment. An apparent red shift of the C=C ethylenic stretching frequency has been found for the ground as well as excited states of retinal-cluster conjugates compared to free retinal (Figure 8 and Table S6). Moreover in the HOOP region, the wagging motions of H–C_{11} and H–C_{12} bonds in opposite direction have been found red shifted too for the ground along with their excited state analogues of the conjugates with respect to free *cis*- and *trans*- retinal (Figure

6.9A, 6.9B, 6.9C, 6.9D and Table S6.6). The intensities of the referred frequencies are also found higher than that of the same for free retinal forms (Figure 6.8 and Figure 6.9A, 6.9B, 6.9C and 6.9D). This indicates the greater degree of deformation of the polyene backbone of retinal in the conjugates than the free retinal isomers. Thus the entire frequency drops with superior intensity in the symmetric stretching mode along with all the hydrogen wagging modes around C_{11}=C_{12} bond implies the large scale backbone distortions of retinal moiety in the conjugates. The changes in vibrational structures thus facilitate the dynamics of rhodopsin to photorhodopsin. This will decrease the force constant value of the H–C_{11}=C_{12}–H bond along with the relevant potential energy barrier for the torsional oscillations. Therefore it is evidenced that the decrease of related forces constants and potential energy barrier of torsional oscillations around the C_{11}=C_{12} double bond facilitates the process of isomerization in the conjugates.

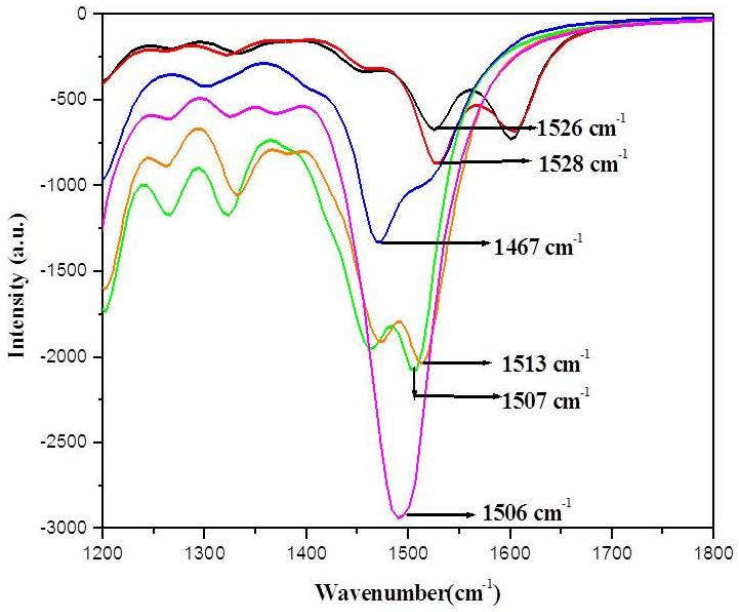

Figure 6.8. The symmetric ethylenic stretching frequency of C_{11}=C_{12} double bond. Here ━ for 11-*cis* retinal, ━ for all-*trans* retinal, ━ for ground state of retinal-gold (O_h) conjugate, ━ for ground state of retinal-gold (D_{2h}) conjugate, ━ for excited state of retinal-gold (O_h) conjugate, ━ for excited state of retinal-gold (D_{2h}) conjugate.

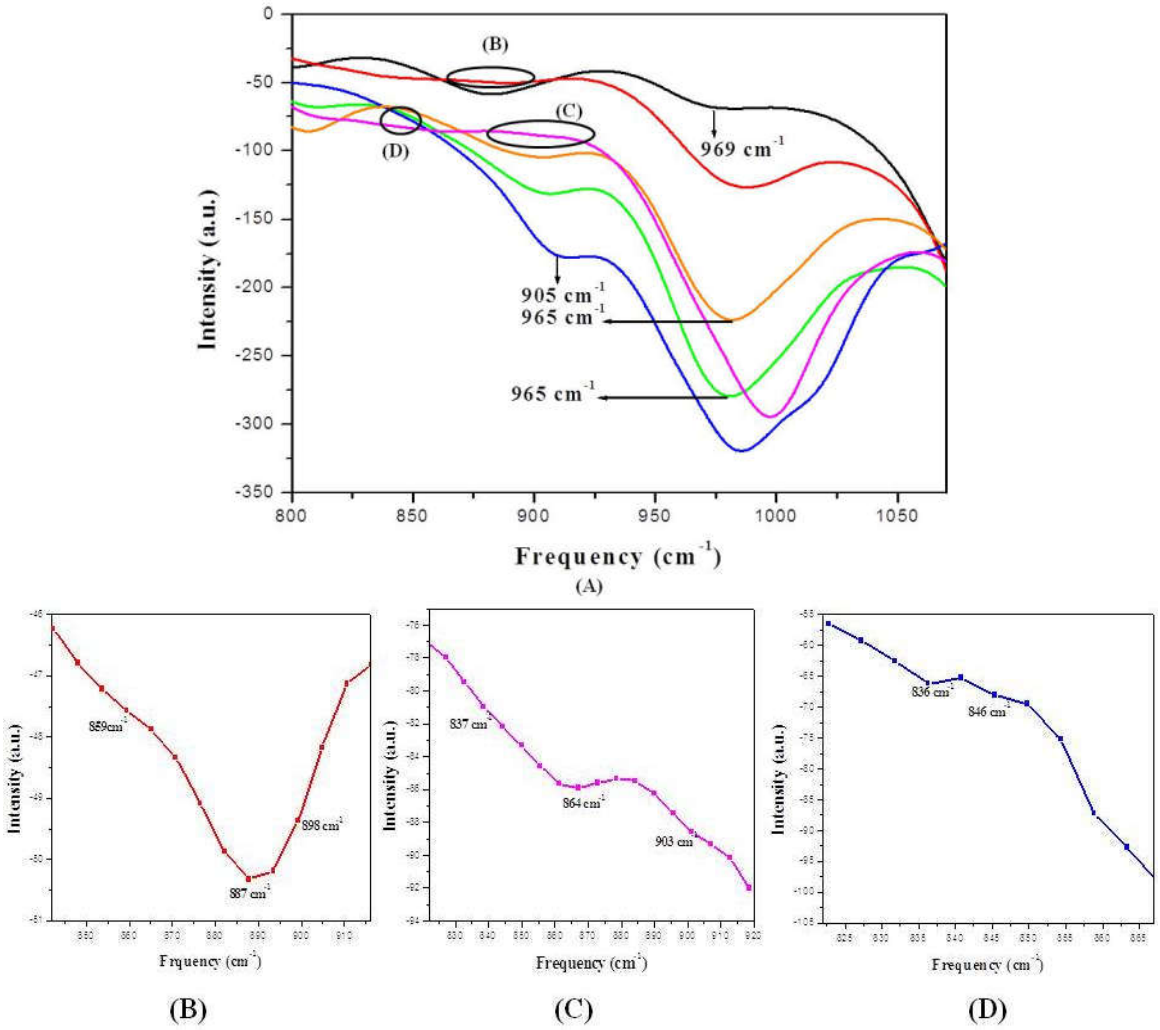

Figure 6.9 **(A)** Frequency of the torsional motion of H–C_{11} and H–C_{12} bond in the HOOP region of C_{11}=C_{12} bond. For better clarification the regions spotted by **(B)**, **(C)**, and **(D)** are amplified individually. Here ▬ for 11-*cis* retinal, ▬ for all-*trans* retinal, ▬ for ground state of retinal-gold (O_h) conjugate, ▬ for ground state of retinal-gold (D_{2h}) conjugate, ▬ for excited state of retinal-gold (O_h) conjugate, ▬ for excited state of retinal-gold (D_{2h}) conjugate.

6.4 Conclusion

The present study imprints the spectral shift of photoisomerization of 11-*cis* retinal while conjugated to Au_{14} nanoclusters of different symmetries. The red shift in the absorption wave lengths of the conjugates recommends for the photoisomerization occurring in the IR region.

This red shift is attributed to the decrease of $E_{occ\text{-}vir}$ value in retinal-gold conjugates with respect to free retinal. Furthermore the excited state estimation of the retinal-cluster conjugates warrants for the occurrence of photoisomerization in the IR region. Being the triggering step of the entire mechanism of vision, the red shifting of this photoisomerization process highlights the possibility of vision enhancement to the IR region. The analysis of major excitations reveals that the absorption in retinal-gold conjugates is due to the charge transfer from gold cluster to retinal molecule. Among all the gold-retinal conjugates, maximum red shifting of the absorption occurs in case of retinal-Au_{14} (O_h). On the other hand, the retinal-Au_{14} (D_{2h}) shows the most intense peak in the absorption profile due to the constructive interference of individual transitions dipole moments. Hence, one can infer this retinal-Au_{14} (D_{2h}) conjugate to be the preeminent elevator of photoisomerization process. The vibrational and subsequent thermochemical analysis of ground states along with the excited states of the conjugates have verified the occurrence as well as spontaneity of photoisomerization of retinal despite of its conjugation with Au_{14} cluster. Finally the speculation of enhancement of vision through the spectral shift of photoisomerization has emerged as the consequence.